Journal of Mathematical Modeling
Vol. 13, No. 4, 2025, pp. 940-962. Research Article

JMM

Numerical study of a two-dimensional eco-epidemiological model with diffusion and convex incidence rate: Unconditionally positivity preserving method

Safieh Bagheri, Mohamad Hossein Akrami, Mohammad Heydari, Ghasem Barid Loghmani*

Department of Mathematical Science, Yazd University, Yazd 89195-741, Iran
Email(s): sbagheri1354@stu.yazd.ac.ir, akrami@yazd.ac.ir, m.heydari@yazd.ac.ir, loghmani@yazd.ac.ir

Abstract. In this paper, a two-dimensional eco-epidemiological model with diffusion and convex incidence rate is studied, that is, the density of population depends on time and two spatial variables. The main challenge in investigation of population models is finding a numerical method to obtain non-negative solutions. Some numerical methods, for instance Euler's method, based on the standard finite difference formulas are inefficient for solving such models because they are not always able to produce non-negative approximate solutions. On the other hand, the non-standard finite difference schemes can provide non-negative approximations conditionally. In the current work, first, the stability of the dynamic proposed eco-epidemiological model is examined. Then, a numerical method that provides unconditional acceptable solutions is introduced. In what follows, the consistency and stability of the numerical method are discussed. Finally, using numerical simulation, the efficiency of this method is compared with the Euler and non-standard methods. Furthermore, we examined the role of initial functions in interpreting species-environment interactions and deliberated on predator-prey behaviors in various scenarios.

Keywords: Consistency, convex incidence rate, eco-epidemiological model, stability, unconditionally positivity preserving method.
AMS Subject Classification 2010: 34A34, 65L05.

1 Introduction

One of the effective techniques for investigating the behavior and disease control of population species is the use of mathematical models [28]. The most powerful and popular mathematical tools for modeling

*Corresponding author
Received: 18 January 2025 / Revised: 10 May 2025 / Accepted: 1 July 2025
DOI: 10.22124/jmm.2025.29603.2634

are the use of differential equations. Partial differential equations (PDEs) are more suitable for describing a system over a realistic time and spatial interval. These equations represent the population distribution by considering the interactions of populations in different locations and time. For example, Holmes et al. discussed the use of PDEs in various models and how to model ecological phenomena in their paper. They also examined the movement patterns of animal species [16]. Dariva and Lepoutre studied the chronic myeloid leukemia disease model. They described their model with PDEs by considering age as a continuous variable and analyzed the stability of the equilibrium points [12]. One of the most useful models employed for analyzing diseases is the family of SIR models. Several important ecological models and their mathematical formulations are summarized in [38]. In the following, we will examine the importance of these models and review previous studies.

1.1 Literature review

Due to the global spread of epidemic diseases, the study of infectious disease models has become increasingly important. Given the significance of preventing and managing infectious diseases, the study of epidemics are considered essential [4]. Buonomo and Lasciategnola examined an SEIR model with convex incidence and analyzed the existence of backward bifurcation. They investigated the global stability of their system by using geometric methods [7]. Cai et al. explored the global dynamics of an SIRS epidemic model with a ratio-dependent incidence rate, along with its corresponding stochastic differential equation [9]. The prevalence of diseases in the environment also poses a risk to human society's health. Consequently, research in the field of eco-epidemiology can simultaneously contribute to improving human health and the environment. Predator-prey models, including the Leslie-Gower model, are commonly employed to analyze ecological dynamics, particularly in disease-impacted systems (e.g., Mondal et al. [27]). Greenhalgh et al. conducted an eco-epidemiological study examining the impact of a disease on a specific species. They investigated the effects of the disease on prey activities, as well as the population densities of both the prey and predator species [15]. Pal and Samanta studied the effects of refuge and disease on the prey species in a predator-prey model and analyzed the dynamic behaviors of the model. They also conducted studies involving discrete time delays in their model [32]. San et al. have considered a model of infectious disease in a periodic environment and conducted research on the speed of wave propagation, travelling wave solution, and the minimum wave speed [39]. In [6], the authors have proposed an eco-epidemiological model with diffusion. They have investigated the travelling wave solutions as well as the effect of preytaxis on the speed of disease invasion and predator attack. Sieber et al. have considered a model of epidemic disease in an animal habitat with intra-group prey competition. They have investigated the effects of disease and pathogens on this competition. Additionally, they have studied changes in the interaction between prey and predator species [42]. In [5], the authors used an epidemic model in the ecosystem with a convex rate and studied the effect of the convexity of the disease transmission function on the speed of predator invasion and different types of prey. Recent advances in eco-epidemiological modeling, including studies on prey-predator systems with harvesting (Saha et al. [36]) and predator switching with prey refuge, have enhanced our understanding of disease-mediated ecological dynamics. These works employ qualitative analysis and control strategies to assess how harvesting and predator behavior influence disease transmission and ecosystem stability [30,31]. Mondal et al. studied a delayed pest-plant ecological model where a disease spreads in the pest population [26].

The transmission rate of a disease in a population is a key factor in mathematical models related to the behavior and spread of a disease in an environment. Initially, the disease prevalence rate was expressed

as a linear function. In order to complete models of various infectious diseases, this rate was modified and presented in a non-linear form (see for example [8, 14, 21, 22]). One of the nonlinear prevalence functions for disease is $\beta I(1+\nu I^{k-1})S$ with $\beta, \nu, k > 0$, introduced by Jin et al. [18]. For $k = 2$, this function named as the convex incidence rate, which is due to the repeated exposure and interaction of an infected person with a susceptible individual, leading to an increase in disease spread [34]. Indeed, convex incidence rate is a non-linear rate of disease prevalence in which the speed of disease transmission increases more rapidly with an increasing number of infected individuals compared to a linear rate, and eventually reaches a constant rate. The increase in disease spread in an environment can be due to the repeated exposure and interaction of an infected person with a susceptible person. For example, respiratory diseases that are transmitted through airborne particles have a higher likelihood of infection compared to the other diseases, and the convex incidence rate can be used in mathematical modeling of such diseases [13, 34]. Din and Algehyne have introduced a model for COVID-19 disease with a convex prevalence rate, and then examined the global stability of the system using the Lyapunov method and local stability by using the Jacobian matrix. They have used a non-standard finite difference method (NS-FDM) in their study for numerical simulation [13]. Khan et al. have conducted research on the model of COVID-19 disease with a convex prevalence rate and its development. They have examined the stability of their model and analyzed the bifurcation by using the central manifold theory [19]. Yang et al. considered a disease delay model with convex incidence rate and studied the stability and existence of Hopf bifurcation [44]. Khan et al. have proposed a model for Hepatitis B disease with a convex prevalence rate and analyzed the stability of their model using Castillo-Chavez and geometric methods. They have developed their model with the help of a control variable and evaluated the system behavior by numerical simulation [20].

Most eco-epidemiological models have been developed with a one-dimensional spatial variable. Recent research emphasizes the importance of cooperative hunting strategies among predators and disease dynamics in prey populations within predator-prey systems [37, 40]. For example, Rahman and Chakravarty modified the eco-epidemiological model introduced by Cosner et al. [11] and investigated the dynamics of equilibrium points and the presence of Hopf bifurcations [33]. Sapoukhina et al. examined the effect of taxis in the predator-prey model, analyzed the system dynamics concerning large-scale predator release. In their model, they employed logistic and Holling Type II response functions [41].

In both human societies and ecosystems, the linear movement of populations appears implausible. Consequently, to develop a model that better mirrors reality, incorporating a higher spatial dimension is a logical approach. Ahmed et al. extensively explored a numerical method for a measles infectious disease model involving spatial diffusion in two dimensions. Their investigation encompassed the analysis of stability and the existence of waves within the proposed model [2].

Given the challenges of obtaining analytical solutions for the majority of eco-epidemiological models, the application of numerical methods becomes essential. Moreover, population models must yield non-negative solutions, as certain existing numerical techniques might result in negative populations. Consequently, researchers in this field are actively seeking numerical methods that generate non-negative solutions to accurately capture the behavior of such models [1, 2, 10, 35].

In the subsequent subsection, we present a two-dimensional predator-prey model that incorporates disease prevalence among the prey species, employing convex incidence rates.

Table 1: The parameters of model (1)

Parameters	**Description**
$\tilde{r}$	Growth rate of the prey species
$\tilde{\sigma}$	Natural mortality rate of preys
d	Natural mortality rate of the predators
$\tilde{\kappa}$	Mortality rate of intergroup prey competition
$\tilde{\alpha}_s$	Predator invasion rate of uninfected prey
$\tilde{\alpha}_i$	Predator invasion rate of infected prey
$\tilde{\mu}$	Disease-related mortality rates for infected prey
e	Predators' conversion rate from prey consumption
$\tilde{d}_s$	Diffusion coefficient of uninfected prey
$\tilde{d}_i$	Diffusion coefficient of infected prey
$\tilde{d}_p$	Diffusion coefficient of predators
$\tilde{\rho}_s$	Time of predator access to sensitive prey
$\tilde{\rho}_i$	Time of predator access to diseased prey
$\tilde{\beta}$	Disease transmission rate from a single contact
$\tilde{\zeta}$	Disease transmission rate double exposures

1.2 Model description and motivation

Here, we consider the following eco-epidemiological model:

$$\begin{cases} \partial_t S = \tilde{d}_s \Delta S + \tilde{r}(S+I) - \tilde{\sigma} S - \tilde{\kappa} S(S+I) - \tilde{\beta} SI(1+\tilde{\zeta} I) - \frac{\tilde{\alpha}_s SP}{1+\tilde{\rho}_s S+\tilde{\rho}_i I}, \\ \partial_t I = \tilde{d}_i \Delta I - (\tilde{\sigma}+\tilde{\mu}) I - \tilde{\kappa} I(S+I) + \tilde{\beta} SI(1+\tilde{\zeta} I) - \frac{\tilde{\alpha}_i IP}{1+\tilde{\rho}_s S+\tilde{\rho}_i I}, \\ \partial_t P = \tilde{d}_p \Delta P - dP + \frac{e(\tilde{\alpha}_s S+\tilde{\alpha}_i I)P}{1+\tilde{\rho}_s S+\tilde{\rho}_i I}, \end{cases} \tag{1}$$

where $\Delta = \frac{\partial^2}{\partial x^2} + \frac{\partial^2}{\partial y^2}$. The initial conditions of (1) are

$$\begin{cases} S(x,y,0) = f_1(x,y), \\ I(x,y,0) = f_2(x,y), \qquad (x,y) \in [0,L_x] \times [0,L_y], \\ P(x,y,0) = f_3(x,y), \end{cases} \tag{2}$$

and the boundary conditions are the homogeneous Neumann conditions. In this system, the functions $f_i(x,y), \quad i = 1,2,3$ are known and also, $S(x,y,t)$, $I(x,y,t)$ and $P(x,y,t)$, respectively, indicate the density of prey infectious, susceptible prey and predator. The non-negative parameters of the model are introduced in Table 1.

Considering that most animals, unlike humans, cannot have self-care methods, the possibility of the interaction of the diseased prey species with susceptible prey is doubled. In other words, animals are directly or indirectly exposed to the disease, and this will cause more spread of the disease among them [19, 20]. For this purpose, we choose a convex disease prevalence rate in our model.
In the proposed model, two-dimensional space is selected to spread animal species in the habitat. The

movement of animals in the habitat can be in different directions. Defending self and escaping the predator, finding food for the weak, chasing and trapping their prey, or facing barriers to nature and closing the path of movement, can be the cause of redirecting the movement of animal species. Therefore, their path of movement is not linear and their movement is on the surface. As a result, models with two-dimensional space can bring us closer to more real results.

On one hand, most eco-epidemiological models are non-linear, making it rarely possible to solve these models analytically. For this reason, many researchers prefer numerical methods to approximate the solutions of these models. On the other hand, sometimes the numerical methods employed to solve non-linear dynamic systems, especially those related to populations, yield unacceptable solutions. This leads to an incorrect analysis of the dynamic behavior of the system. While a system may not inherently behave chaotically, certain numerical methods result in chaotic solutions [2]. Given the nuanced nature of population models, attaining positive solutions is crucial. Negative solutions in such models lead to unrealistic fluctuations. Therefore, we are in search of numerical methods that, in addition to producing positive solutions, provide a reliable approximation of the solution. One of the most widely recommended numerical methods for approximating PDEs is the finite difference method (FDM) [17, 23, 25]. In this work, using the FDM, we propose a technique that can identify a positive solution. The subsequent section outlines the structure of this study.

1.3 Structure of the paper

This paper is organized as follows: In Section 2, the stability of equilibria is examined. Section 3, is related to the explanation of numerical methods. The consistency of the proposed numerical method is analyzed in Section 4 . Then, the stability of the proposed FDM is discussed in Section 5. Numerical simulations based on the proposed method are provided in Section 6. Finally, the conclusion are summarized in the last section.

2 The stability of equilibria

In this section, the stability of equilibria is examined. To simplify numerical and dynamic analysis, we define

$$\begin{cases} \varphi_1(S,I) = \tilde{r}(S+I), \\ \varphi_2(S,I) = \tilde{\sigma} + \tilde{\kappa}(S+I), \\ \varphi_3(S,I) = (\tilde{\sigma}+\tilde{\mu}) + \tilde{\kappa}(S+I), \\ \varphi_4(I) = \tilde{\beta} I(1+\tilde{\zeta} I), \\ \varphi_5(S,I,P) = \frac{P}{1+\tilde{\rho}_s S+\tilde{\rho}_i I}, \end{cases} \tag{3}$$

where, the functions $\varphi_1, \varphi_2, \varphi_3, \varphi_4, \varphi_5$ represent the growth rate of prey, death rate of susceptible, death rate of infected prey, incidence rate and functional response, respectively. Using relation (3) and for simplicity of calculations, system (1) is rewritten as follows:

$$\begin{cases} \partial_t S = \tilde{d}_s \Delta S + \varphi_1(S,I) - \varphi_2(S,I)S - \varphi_4(I)S - \tilde{\alpha}_s \varphi_5(S,I,P)S, \\ \partial_t I = \tilde{d}_i \Delta I - \varphi_3(S,I)I + \varphi_4(I)S - \tilde{\alpha}_i \varphi_5(S,I,P)I, \\ \partial_t P = \tilde{d}_p \Delta P - dP + e\left(\tilde{\alpha}_s S + \tilde{\alpha}_i I\right)\varphi_5(S,I,P). \end{cases} \tag{4}$$

The equilibrium point (S^*, I^*, P^*) is obtained by solving the following system of equations:

$$\begin{cases} \tilde{d}_s \Delta S + \varphi_1(S,I) - \varphi_2(S,I)S - \varphi_4(I)S - \tilde{\alpha}_s S \varphi_5(S,I,P) = 0, \\ \tilde{d}_i \Delta I - \varphi_3(S,I)I + \varphi_4(I)S - \tilde{\alpha}_i I \varphi_5(S,I,P) = 0, \\ \tilde{d}_p \Delta P - dP + e\big(\tilde{\alpha}_s S + \tilde{\alpha}_i I\big)\varphi_5(S,I,P) = 0. \end{cases}$$

Consider the following linear system around the equilibrium point (S^*, I^*, P^*):

$$\begin{cases} \partial_t S = \tilde{d}_s \Delta S + a_{11} S + a_{12} I + a_{13} P, \\ \partial_t I = \tilde{d}_i \Delta I + a_{21} S + a_{22} I + a_{23} P, \\ \partial_t P = \tilde{d}_p \Delta P + a_{31} S + a_{32} I + a_{33} P, \end{cases} \tag{5}$$

where, the values of a_{mn}, $m,n = 1,2,3$ are obtained as follows:

$$\begin{aligned} a_{11} &= -\tilde{\alpha}_s S^* \partial_s \varphi_5(S^*,I^*,P^*) - \tilde{\alpha}_s \varphi_5(S^*,I^*,P^*) - \tilde{\beta}\tilde{\xi} I^{*^2} - (\tilde{\beta} + \tilde{\kappa}) I^* - 2\tilde{\kappa} S^* + \tilde{r} - \tilde{\sigma}, \\ a_{12} &= -\tilde{\alpha}_s \partial_i S^* \varphi_5(S^*,I^*,P^*) + \big(-2\tilde{\beta}\tilde{\xi} I^* - \tilde{\beta} - \tilde{\kappa}\big) S^* + \tilde{r}, \\ a_{13} &= -\tilde{\alpha}_s S^* \partial_p \varphi_5(S^*,I^*,P^*), \\ a_{21} &= I^* \big(\tilde{\beta}\tilde{\xi} I^* - \tilde{\alpha}_i \partial_s \varphi_5(S^*,I^*,P^*) + \tilde{\beta} - \tilde{\kappa}\big), \\ a_{22} &= -\tilde{\alpha}_i I^* \partial_i \varphi_5(S^*,I^*,P^*) - \tilde{\alpha}_i \varphi_5(S^*,I^*,P^*) + \big(2\tilde{\beta}\tilde{\xi} S^* - 2\tilde{\kappa}\big) I^* + \big(\tilde{\beta} - \tilde{\kappa}\big) S^* - \tilde{\mu} - \tilde{\sigma}, \\ a_{23} &= -\tilde{\alpha}_i I^* \partial_p \varphi_5(S^*,I^*,P^*), \\ a_{31} &= e\big(\tilde{\alpha}_i I^* + \tilde{\alpha}_s S^*\big) \partial_s \varphi_5(S^*,I^*,P^*) + e\tilde{\alpha}_s \varphi_5(S^*,I^*,P^*), \\ a_{32} &= e\big(\tilde{\alpha}_i I^* + \tilde{\alpha}_s S^*\big) \partial_i \varphi_5(S^*,I^*,P^*) + e\tilde{\alpha}_i \varphi_5(S^*,I^*,P^*), \\ a_{33} &= -d + e\big(\tilde{\alpha}_i I^* + \tilde{\alpha}_s S^*\big) \partial_p \varphi_5(S^*,I^*,P^*). \end{aligned}$$

Suppose the solutions of system (5) are in the form of Fourier series, that is:

$$\begin{aligned} S(x,y,t) &= \sum_{l,k} S_{l,k} e^{\lambda t} \cos(lx)\cos(ky), \\ I(x,y,t) &= \sum_{l,k} I_{l,k} e^{\lambda t} \cos(lx)\cos(ky), \\ P(x,y,t) &= \sum_{l,k} P_{l,k} e^{\lambda t} \cos(lx)\cos(ky), \end{aligned}$$

where $l = \frac{n_1 \pi}{2}$ and $k = \frac{n_2 \pi}{2}$ $(n_1, n_2 \in \mathbb{N})$ are the wave numbers. Putting $S(x,y,t)$, $I(x,y,t)$ and $P(x,y,t)$ in system (5), we have

$$\begin{cases} \big(a_{11} - \tilde{d}_s l^2 - \tilde{d}_s k^2 - \lambda\big) S + a_{12} I + a_{13} P = 0, \\ a_{21} S + \big(a_{22} - \tilde{d}_i l^2 - \tilde{d}_i k^2 - \lambda\big) I + a_{23} P = 0, \\ a_{31} S + a_{32} I + \big(a_{33} - \tilde{d}_p l^2 - \tilde{d}_p k^2 - \lambda\big) P = 0. \end{cases} \tag{6}$$

Based on the Roth-Horwitz stability criterion, consider the characteristic polynomial of system (6):

$$\lambda^3 + \omega_2(l,k)\lambda^2 + \omega_1(l,k)\lambda + \omega_0(l,k) = 0,$$

where

$$\begin{aligned}
\omega_2(l,k) &= (\tilde{d}_i+\tilde{d}_p+\tilde{d}_s)k^2+(\tilde{d}_i+\tilde{d}_p+\tilde{d}_s)l^2-a_{22}-a_{33}-a_{11},\\
\omega_1(l,k) &= \big((\tilde{d}_p+\tilde{d}_s)\tilde{d}_i+\tilde{d}_p\tilde{d}_s\big)k^4+\big[\big((2\tilde{d}_p+2\tilde{d}_s)\tilde{d}_i+2\tilde{d}_p\tilde{d}_s\big)l^2+(-a_{33}-a_{11})\tilde{d}_i+(-a_{22}-a_{11})\tilde{d}_p\\
&\quad-\tilde{d}_s(a_{22}+a_{33})\big]k^2+\big((\tilde{d}_p+\tilde{d}_s)\tilde{d}_i+\tilde{d}_p\tilde{d}_s\big)l^4+\big((-a_{33}-a_{11})\tilde{d}_i-(a_{22}+a_{11})\tilde{d}_p\\
&\quad-\tilde{d}_s(a_{22}+a_{33})\big)l^2+(a_{22}+a_{33})a_{11}-a_{12}a_{21}+a_{22}a_{33}-a_{23}a_{32}-a_{13}a_{31},\\
\omega_0(l,k) &= k^6\tilde{d}_i\tilde{d}_p\tilde{d}_s+\big(3l^2\tilde{d}_i\tilde{d}_p\tilde{d}_s+(-a_{11}\tilde{d}_p-a_{33}\tilde{d}_s)\tilde{d}_i-a_{22}\tilde{d}_p\tilde{d}_s\big)k^4+\big[3l^4\tilde{d}_i\tilde{d}_p\tilde{d}_s+\big((-2a_{11}\tilde{d}_p\\
&\quad-2a_{33}\tilde{d}_s)\tilde{d}_i-2a_{22}\tilde{d}_p\tilde{d}_s\big)l^2+(a_{11}a_{33}-a_{13}a_{31})\tilde{d}_i+(a_{11}a_{22}-a_{12}a_{21})\tilde{d}_p\\
&\quad+\tilde{d}_s(a_{22}a_{33}-a_{23}a_{32})\big]k^2+l^6\tilde{d}_i\tilde{d}_p\tilde{d}_s+\big((-a_{11}\tilde{d}_p-a_{33}\tilde{d}_s)\tilde{d}_i-a_{22}\tilde{d}_p\tilde{d}_s\big)l^4\\
&\quad+\big((a_{11}a_{33}-a_{13}a_{31})\tilde{d}_i+(a_{11}a_{22}-a_{12}a_{21})\tilde{d}_p+\tilde{d}_s(a_{22}a_{33}-a_{23}a_{32})\big)l^2\\
&\quad+(a_{23}a_{32}-a_{22}a_{33})a_{11}-a_{13}a_{21}a_{32}+a_{12}a_{21}a_{33}+a_{13}a_{22}a_{31}-a_{12}a_{23}a_{31}.
\end{aligned}$$

Therefore, system (4) at endemic equilibrium point (S^*,I^*,P^*) is stable under the conditions

$$\begin{cases}
\omega_2(l,k)>0,\\
\omega_0(l,k)>0,\\
\omega_2(l,k)\omega_1(l,k)-\omega_0(l,k)>0.
\end{cases} \tag{7}$$

Considering the large number of parameters and the difficulty of finding their analytical relationships, we can numerically investigate the stability of equilibrium points by selecting specific values of the parameters in certain cases. Here, by choosing parameters $\tilde{r}=0.4$, $\tilde{\sigma}=0.03$, $\tilde{d}=0.45$, $\tilde{\kappa}=0.2$, $\tilde{\alpha}_s=1$, $\tilde{\alpha}_i=1$, $\tilde{\mu}=0.3$, $\tilde{e}=1$, $\tilde{d}_s=0$, $\tilde{d}_i=0$, $\tilde{d}_p=0$, $\tilde{\rho}_s=0.3$, $\tilde{\rho}_i=0.3$, $\tilde{\beta}=1.5$ and $\tilde{\zeta}=0.3$, system (4) has five acceptable equilibrium points as:

- $E_1=\big(0,\ 0,\ 0\big)$ is trivial equilibrium point,
- $E_2=\big(1.233333333,\ 0,\ 0\big)$ is prey equilibrium point,
- $E_3=\big(0.5882352941,\ 0,\ 0.2276816609\big)$ is disease free equilibrium point,
- $E_4=\big(0.3231552167,\ 0.3738271639,\ 0\big)$ is only prey equilibrium point,
- $E_5=\big(0.36714387,\ 0.2210914174,\ 0.09502681046\big)$ is endemic equilibrium point.

Using conditions (7), the stability of equilibrium points of system (4) is shown in Table 2.
To solve model (4), we will describe the following three numerical methods:

- Forward Euler finite difference method (FE-FDM),
- NS-FDM,
- Unconditionally positivity preserving FDM (UPP-FDM).

According to the nature of population system (4), the solutions must be non-negative. We use these three FDMs to approximate the solutions of system (4) to test whether these methods can produce non-negative solutions or not.

Table 2: The stability of equilibrium points

Equ. Points	ω_2	ω_0	$\omega_1\omega_2-\omega_0$	Stability
E_1	0.46	−0.06105	−0.004316	×
E_2	−1.180243309	0.1703035278	−0.0365699001	×
E_3	−0.03491176480	−0.01499852942	0.01306568607	×
E_4	0.5410045428	−0.01382794090	0.08614504247	×
E_5	0.3687042477	0.007015001256	0.04395782533	✓

3 Description of numerical methods

One of the most popular techniques for the numerical solution of PDEs is the FDM. In this method, by using derivative approximations, the continuous system converts into a discrete model in its domain. Here, we discretize the range of time and space variables uniformly. To construct FDM, choose integers $M_x,\ M_y,\ N>0$ and let $h_x=\frac{L_x}{M_x},\ h_y=\frac{L_y}{M_y}$ and $\tau=\frac{T}{N}$. Also, define

$$\Omega_{h_x}=\{x_i : x_i=ih_x,\ 0\le i\le M_x\}, \tag{8}$$
$$\Omega_{h_y}=\{y_j : y_j=jh_y,\ 0\le j\le M_y\}, \tag{9}$$
$$\Omega_{\tau}=\{t_n : t_n=n\tau,\ 0\le n\le N\}. \tag{10}$$

Assuming that $U^n_{i,j}$ is an approximation of $U(x_i,y_j,t_n)$, we use the following notations to make it easier to develop the method:

$$\delta_\tau U^n_{i,j}=\frac{1}{\tau}\left[U^{n+1}_{i,j}-U^n_{i,j}\right], \tag{11}$$
$$\tilde{\delta}_{h_x} U^n_{i,j}=\frac{1}{2h_x}\left[U^n_{i+1,j}-U^n_{i-1,j}\right], \tag{12}$$
$$\tilde{\delta}_{h_y} U^n_{i,j}=\frac{1}{2h_y}\left[U^n_{i,j+1}-U^n_{i,j-1}\right], \tag{13}$$
$$\Delta_{h_x} U^n_{i,j}=\frac{1}{{h_x}^2}\left[U^n_{i+1,j}-2U^n_{i,j}+U^n_{i-1,j}\right], \tag{14}$$
$$\Delta_{h_y} U^n_{i,j}=\frac{1}{{h_y}^2}\left[U^n_{i,j+1}-2U^n_{i,j}+U^n_{i,j-1}\right]. \tag{15}$$

3.1 FE-FDM

Substituting mesh points (8)-(10) into system (4) and applying formulas (11), (14), and (15), we derive the following set of discrete equations:

$$\begin{cases} \delta_\tau S^n_{i,j}=\tilde{d}_s\left(\Delta_{h_x}S^n_{i,j}+\Delta_{h_y}S^n_{i,j}\right)+\varphi_1(S^n_{i,j},I^n_{i,j})-S^n_{i,j}\left(\varphi_2(S^n_{i,j},I^n_{i,j})+\varphi_4(I^n_{i,j})+\tilde{\alpha}_s\varphi_5(S^n_{i,j},I^n_{i,j},P^n_{i,j})\right),\\ \delta_\tau I^n_{i,j}=\tilde{d}_i\left(\Delta_{h_x}I^n_{i,j}+\Delta_{h_y}I^n_{i,j}\right)-I^n_{i,j}\varphi_3(S^n_{i,j},I^n_{i,j})+S^n_{i,j}\varphi_4(I^n_{i,j})-\tilde{\alpha}_i I^n_{i,j}\varphi_5(S^n_{i,j},I^n_{i,j},P^n_{i,j}),\\ \delta_\tau P^n_{i,j}=\tilde{d}_p\left(\Delta_{h_x}P^n_{i,j}+\Delta_{h_y}P^n_{i,j}\right)-dP^n_{i,j}+e\left(\tilde{\alpha}_s S^n_{i,j}+\tilde{\alpha}_i I^n_{i,j}\right)\varphi_5(S^n_{i,j},I^n_{i,j},P^n_{i,j}), \end{cases} \tag{16}$$

for $0 \le i \le M_x$, $0 \le j \le M_y$ and $0 \le n \le N-1$. Therefore, with the FE-FDM, we arrive at the following explicit formulas:

$$\begin{cases} S_{i,j}^{n+1} = \big(1-2\gamma_{s_x}-2\gamma_{s_y}\big)S_{i,j}^{n} + \gamma_{s_x}\big(S_{i+1,j}^{n}+S_{i-1,j}^{n}\big) + \gamma_{s_y}\big(S_{i,j+1}^{n}+S_{i,j-1}^{n}\big) + \tau\big[\varphi_1(S_{i,j}^{n},I_{i,j}^{n}) \\ \qquad -S_{i,j}^{n}\varphi_2(S_{i,j}^{n},I_{i,j}^{n}) - S_{i,j}^{n}\varphi_4(I_{i,j}^{n}) - \tilde{\alpha}_s S_{i,j}^{n}\varphi_5(S_{i,j}^{n},I_{i,j}^{n},P_{i,j}^{n})\big], \\ I_{i,j}^{n+1} = \big(1-2\gamma_{i_x}-2\gamma_{i_y}\big)I_{i,j}^{n} + \gamma_{i_x}\big(I_{i+1,j}^{n}+I_{i-1,j}^{n}\big) + \gamma_{s_i}\big(I_{i,j+1}^{n}+I_{i,j-1}^{n}\big) + \tau\big[-I_{i,j}^{n}\varphi_3(S_{i,j}^{n},I_{i,j}^{n}) \\ \qquad +S_{i,j}^{n}\varphi_4(I_{i,j}^{n}) - \tilde{\alpha}_i I_{i,j}^{n}\varphi_5(S_{i,j}^{n},I_{i,j}^{n},P_{i,j}^{n})\big], \\ P_{i,j}^{n+1} = \big(1-2\gamma_{p_x}-2\gamma_{p_y}\big)P_{i,j}^{n} + \gamma_{p_x}\big(P_{i+1,j}^{n}+P_{i-1,j}^{n}\big) + \gamma_{p_y}\big(P_{i,j+1}^{n}+P_{i,j-1}^{n}\big) + \tau\big[-dP_{i,j}^{n} \\ \qquad +e\big(\tilde{\alpha}_s S_{i,j}^{n}+\tilde{\alpha}_i I_{i,j}^{n}\big)\varphi_5(S_{i,j}^{n},I_{i,j}^{n},P_{i,j}^{n})\big], \end{cases} \tag{17}$$

where

$$\gamma_{s_x} = \frac{\tau\tilde{d}_s}{{h_x}^2},\ \gamma_{s_y} = \frac{\tau\tilde{d}_s}{{h_y}^2},\ \gamma_{i_x} = \frac{\tau\tilde{d}_i}{{h_x}^2},\ \gamma_{i_y} = \frac{\tau\tilde{d}_i}{{h_y}^2},\ \gamma_{p_x} = \frac{\tau\tilde{d}_p}{{h_x}^2},\ \gamma_{p_y} = \frac{\tau\tilde{d}_p}{{h_y}^2}. \tag{18}$$

Using the initial conditions (2), the initial conditions of the discrete model are computed in the following form:

$$\begin{cases} S_{i,j}^{0} = f_1(x_i,y_j), & 0 \le i \le M_x,\ 0 \le j \le M_y, \\ I_{i,j}^{0} = f_2(x_i,y_j), & 0 \le i \le M_x,\ 0 \le j \le M_y, \\ P_{i,j}^{0} = f_3(x_i,y_j) & 0 \le i \le M_x,\ 0 \le j \le M_y. \end{cases} \tag{19}$$

Now, employing the boundary conditions

$$\partial_x S(0,y,t) = \partial_x S(L_x,y,t) = \partial_x S(x,0,t) = \partial_x S(x,L_y,t) = 0,$$

and the formulas (12) and (13), give

$$\tilde{\delta}_{h_x} S_{0,j}^{n} = \frac{1}{2h_x}\big[S_{1,j}^{n} - S_{-1,j}^{n}\big],$$

$$\tilde{\delta}_{h_y} S_{i,0}^{n} = \frac{1}{2h_y}\big[S_{i,1}^{n} - S_{i,-1}^{n}\big].$$

So, for $0 \le i \le M_x$, $0 \le j \le M_y$ and $0 \le n \le N$, we have $S_{1,j}^{n} = S_{-1,j}^{n}$ and $S_{i,1}^{n} = S_{i,-1}^{n}$. Similarly, we can derive that $I_{1,j}^{n} = I_{-1,j}^{n}$, $I_{i,1}^{n} = I_{i,-1}^{n}$, $P_{1,j}^{n} = P_{-1,j}^{n}$ and $P_{i,1}^{n} = P_{i,-1}^{n}$.

Consider in mind, based on (17), it is very difficult to control the solutions in FE-FDM.

3.2 NS-FDM

In this subsection, according to the scheme proposed by Mickens [24], we construct the NS-FDM on the system (4) as follows:

$$\begin{cases} S_{i,j}^{n+1} = S_{i,j}^{n} + \gamma_{s_x}\big[S_{i+1,j}^{n} - 2S_{i,j}^{n} + S_{i-1,j}^{n}\big] + \gamma_{s_y}\big[S_{i,j+1}^{n} - 2S_{i,j}^{n} + S_{i,j-1}^{n}\big] + \tau\big[\varphi_1(S_{i,j}^{n},I_{i,j}^{n}) \\ \qquad -S_{i,j}^{n+1}\varphi_2(S_{i,j}^{n},I_{i,j}^{n}) - S_{i,j}^{n+1}\varphi_4(I_{i,j}^{n}) - \tilde{\alpha}_s S_{i,j}^{n+1}\varphi_5(S_{i,j}^{n},I_{i,j}^{n},P_{i,j}^{n})\big], \\ I_{i,j}^{n+1} = I_{i,j}^{n} + \gamma_{i_x}\big(I_{i+1,j}^{n} - 2I_{i,j}^{n} + I_{i-1,j}^{n}\big) + \gamma_{s_i}\big(I_{i,j+1}^{n} - 2I_{i,j}^{n} + I_{i,j-1}^{n}\big) + \tau\big[-I_{i,j}^{n+1}\varphi_3(S_{i,j}^{n},I_{i,j}^{n}) \\ \qquad +S_{i,j}^{n}\varphi_4(I_{i,j}^{n}) - \tilde{\alpha}_i I_{i,j}^{n+1}\varphi_5(S_{i,j}^{n},I_{i,j}^{n},P_{i,j}^{n})\big], \\ P_{i,j}^{n+1} = P_{i,j}^{n} + \gamma_{p_x}\big(P_{i+1,j}^{n} - 2P_{i,j}^{n} + P_{i-1,j}^{n}\big) + \gamma_{p_y}\big(P_{i,j+1}^{n} - 2P_{i,j}^{n} + P_{i,j-1}^{n}\big) + \tau\big[-dP_{i,j}^{n+1} \\ \qquad +e\big(\tilde{\alpha}_s S_{i,j}^{n} + \tilde{\alpha}_i I_{i,j}^{n}\big) \times \varphi_5(S_{i,j}^{n},I_{i,j}^{n},P_{i,j}^{n})\big]. \end{cases} \tag{20}$$

After rewriting and categorizing the sentences, we have

$$\begin{cases} S_{i,j}^{n+1}\left[1+\tau\varphi_2(S_{i,j}^n,I_{i,j}^n)+\tau\varphi_4(I_{i,j}^n+\tau\tilde{\alpha}_s\varphi_5(S_{i,j}^n,I_{i,j}^n,P_{i,j}^n))\right]=\left(1-2\gamma_{s_x}-2\gamma_{s_y}\right)S_{i,j}^n \\ \quad +\gamma_{s_x}\left(S_{i+1,j}^n+S_{i-1,j}^n\right)+\gamma_{s_y}\left(S_{i,j+1}^n+S_{i,j-1}^n\right)+\tau\varphi_1(S_{i,j}^n,I_{i,j}^n)], \\ I_{i,j}^{n+1}\left[1+\tau\varphi_3(S_{i,j}^n,I_{i,j}^n)+\tau\tilde{\alpha}_i\varphi_5(S_{i,j}^n,I_{i,j}^n,P_{i,j}^n)\right]=\left(1-2\gamma_{i_x}-2\gamma_{i_y}\right)I_{i,j}^n+\gamma_{i_x}\left(I_{i+1,j}^n\right. \\ \quad \left.+I_{i-1,j}^n\right)+\gamma_{s_i}\left(I_{i,j+1}^n+I_{i,j-1}^n\right)+\tau\varphi_4(I_{i,j}^n)S_{i,j}^n, \\ P_{i,j}^{n+1}\left[1+d\right]=\left(1-2\gamma_{p_x}-2\gamma_{p_y}\right)P_{i,j}^n+\gamma_{p_x}\left(P_{i+1,j}^n+P_{i-1,j}^n\right)+\gamma_{p_y}\left(P_{i,j+1}^n+\tau e\left(\tilde{\alpha}_s S_{i,j}^n\right.\right. \\ \quad \left.\left.+\tilde{\alpha}_i I_{i,j}^n\right)+P_{i,j-1}^n\right)\varphi_5(S_{i,j}^n,I_{i,j}^n,P_{i,j}^n). \end{cases} \tag{21}$$

Finally, utilizing (21), the following explicit formulas are obtained:

$$\begin{cases} S_{i,j}^{n+1}=\frac{1}{AN_1}\left[\left(1-2\gamma_{s_x}-2\gamma_{s_y}\right)S_{i,j}^n+\gamma_{s_x}\left(S_{i+1,j}^n+S_{i-1,j}^n\right)+\gamma_{s_y}\left(S_{i,j+1}^n+S_{i,j-1}^n\right)+\tau\varphi_1(S_{i,j}^n,I_{i,j}^n)\right], \\ I_{i,j}^{n+1}=\frac{1}{AN_2}\left[\left(1-2\gamma_{i_x}-2\gamma_{i_y}\right)I_{i,j}^n+\gamma_{i_x}\left(I_{i+1,j}^n+I_{i-1,j}^n\right)+\gamma_{s_i}\left(I_{i,j+1}^n+I_{i,j-1}^n\right)+\tau\varphi_4(I_{i,j}^n)S_{i,j}^n\right], \\ P_{i,j}^{n+1}=\frac{1}{AN_3}\left[\left(1-2\gamma_{p_x}-2\gamma_{p_y}\right)P_{i,j}^n+\gamma_{p_x}\left(P_{i+1,j}^n+P_{i-1,j}^n\right)+\gamma_{p_y}\left(P_{i,j+1}^n+P_{i,j-1}^n\right)+\tau e\left(\tilde{\alpha}_s S_{i,j}^n\right.\right. \\ \quad \left.\left.+\tilde{\alpha}_i I_{i,j}^n\right)\varphi_5(S_{i,j}^n,I_{i,j}^n,P_{i,j}^n)\right], \end{cases} \tag{22}$$

where

$$\begin{aligned} AN_1 &= 1+\tau\varphi_2(S_{i,j}^n,I_{i,j}^n)+\tau\varphi_4(I_{i,j}^n+\tau\tilde{\alpha}_s\varphi_5(S_{i,j}^n,I_{i,j}^n,P_{i,j}^n)), \\ AN_2 &= 1+\tau\varphi_3(S_{i,j}^n,I_{i,j}^n)+\tau\tilde{\alpha}_i\varphi_5(S_{i,j}^n,I_{i,j}^n,P_{i,j}^n), \\ AN_3 &= 1+d. \end{aligned}$$

Similarly, the initial and boundary conditions are calculated as method FE-FDM in Subsection 3.1. According to (22), the approximations obtained by the NS-FDM are positive if

$$\begin{cases} 1-2\gamma_{s_x}-2\gamma_{s_y}>0, \\ 1-2\gamma_{i_x}-2\gamma_{i_y}>0, \\ 1-2\gamma_{p_x}-2\gamma_{p_y}>0. \end{cases} \tag{23}$$

Putting relations (18) into (23) and rewriting them, we have

$$\begin{cases} \frac{{h_x}^2{h_y}^2}{{h_x}^2+{h_y}^2}>2\tau\tilde{d}_s, \\ \frac{{h_x}^2{h_y}^2}{{h_x}^2+{h_y}^2}>2\tau\tilde{d}_i, \\ \frac{{h_x}^2{h_y}^2}{{h_x}^2+{h_y}^2}>2\tau\tilde{d}_p. \end{cases} \tag{24}$$

Therefore, the divisions of space and time can be chosen according to conditions (24), so that the solutions are positive.

3.3 UPP-FDM

Considering that the two numerical methods presented in the previous subsections may produce a negative solution, therefore, according to Ahmed's proposed method [2], we present the unconditionally

positivity preserving method for model (4), as

$$\begin{cases} S_{i,j}^{n+1} = S_{i,j}^{n} + \gamma_{s_x}\left[S_{i+1,j}^{n} - 2S_{i,j}^{n+1} + S_{i-1,j}^{n}\right] + \gamma_{s_y}\left[S_{i,j+1}^{n} - 2S_{i,j}^{n+1} + S_{i,j-1}^{n}\right] + \tau\left[\varphi_1(S_{i,j}^{n}, I_{i,j}^{n})\right. \\ \quad \left. - S_{i,j}^{n+1}\varphi_2(S_{i,j}^{n}, I_{i,j}^{n}) - S_{i,j}^{n+1}\varphi_4(I_{i,j}^{n}) - \tilde{\alpha}_s S_{i,j}^{n+1}\varphi_5(S_{i,j}^{n}, I_{i,j}^{n}, P_{i,j}^{n})\right], \\ I_{i,j}^{n+1} = I_{i,j}^{n} + \gamma_{i_x}\left(I_{i+1,j}^{n} - 2I_{i,j}^{n+1} + I_{i-1,j}^{n}\right) + \gamma_{s_i}\left(I_{i,j+1}^{n} - 2I_{i,j}^{n+1} + I_{i,j-1}^{n}\right) + \tau\left[-I_{i,j}^{n+1}\varphi_3(S_{i,j}^{n}, I_{i,j}^{n})\right. \\ \quad \left. + S_{i,j}^{n}\varphi_4(I_{i,j}^{n}) - \tilde{\alpha}_i I_{i,j}^{n+1}\varphi_5(S_{i,j}^{n}, I_{i,j}^{n}, P_{i,j}^{n})\right], \\ P_{i,j}^{n+1} = P_{i,j}^{n} + \gamma_{p_x}\left(P_{i+1,j}^{n} - 2P_{i,j}^{n+1} + P_{i-1,j}^{n}\right) + \gamma_{p_y}\left(P_{i,j+1}^{n} - 2P_{i,j}^{n+1} + P_{i,j-1}^{n}\right) + \tau\left[-dP_{i,j}^{n+1}\right. \\ \quad \left. + e\left(\tilde{\alpha}_s S_{i,j}^{n} + \tilde{\alpha}_i I_{i,j}^{n}\right)\varphi_5(S_{i,j}^{n}, I_{i,j}^{n}, P_{i,j}^{n})\right]. \end{cases} \tag{25}$$

Arranging the terms of the discrete equations, the following explicit and non-negative formulas are obtained:

$$\begin{cases} S_{i,j}^{n+1}\left[1 + 2\gamma_{s_x} + 2\gamma_{s_y} + \tau\varphi_2(S_{i,j}^{n}, I_{i,j}^{n}) + \tau\varphi_4(I_{i,j}^{n}) + \tau\tilde{\alpha}_s\varphi_5(S_{i,j}^{n}, I_{i,j}^{n}, P_{i,j}^{n})\right] = S_{i,j}^{n} + \gamma_{s_x} \\ \quad \times\left(S_{i+1,j}^{n} + S_{i-1,j}^{n}\right) + \gamma_{s_y}\left(S_{i,j+1}^{n} + S_{i,j-1}^{n}\right) + \tau\varphi_1(S_{i,j}^{n}, I_{i,j}^{n}), \\ I_{i,j}^{n+1}\left[1 + 2\gamma_{i_x} + 2\gamma_{i_y} + \tau\varphi_3(S_{i,j}^{n}, I_{i,j}^{n}) + \tau\tilde{\alpha}_i\varphi_5(S_{i,j}^{n}, I_{i,j}^{n}, P_{i,j}^{n})\right] = I_{i,j}^{n} + \gamma_{i_x}\left(I_{i+1,j}^{n} + I_{i-1,j}^{n}\right) \\ \quad + \gamma_{s_i}\left(I_{i,j+1}^{n} + I_{i,j-1}^{n}\right) + \tau\varphi_4(I_{i,j}^{n})S_{i,j}^{n}, \\ P_{i,j}^{n+1}\left[1 + 2\gamma_{p_x} + 2\gamma_{p_y} + \tau d\right] = P_{i,j}^{n} + \gamma_{p_x}\left(P_{i+1,j}^{n} + P_{i-1,j}^{n}\right) + \gamma_{p_y}\left(P_{i,j+1}^{n} + P_{i,j-1}^{n}\right) + \tau e \\ \quad \times\left(\tilde{\alpha}_s S_{i,j}^{n} + \tilde{\alpha}_i I_{i,j}^{n}\right)\varphi_5(S_{i,j}^{n}, I_{i,j}^{n}, P_{i,j}^{n}). \end{cases} \tag{26}$$

The relation (26) can be simplified as follows:

$$\begin{cases} S_{i,j}^{n+1} = \frac{1}{AP_1}\left[S_{i,j}^{n} + \gamma_{s_x}\left(S_{i+1,j}^{n} + S_{i-1,j}^{n}\right) + \gamma_{s_y}\left(S_{i,j+1}^{n} + S_{i,j-1}^{n}\right) + \tau\varphi_1(S_{i,j}^{n}, I_{i,j}^{n})\right], \\ I_{i,j}^{n+1} = \frac{1}{AP_2}\left[I_{i,j}^{n} + \gamma_{i_x}\left(I_{i+1,j}^{n} + I_{i-1,j}^{n}\right) + \gamma_{s_i}\left(I_{i,j+1}^{n} + I_{i,j-1}^{n}\right) + \tau\varphi_4(I_{i,j}^{n})S_{i,j}^{n}\right], \\ P_{i,j}^{n+1} = \frac{1}{AP_3}\left[P_{i,j}^{n} + \gamma_{p_x}\left(P_{i+1,j}^{n} + P_{i-1,j}^{n}\right) + \gamma_{p_y}\left(P_{i,j+1}^{n} + P_{i,j-1}^{n}\right) + \tau e\left(\tilde{\alpha}_s S_{i,j}^{n}\right.\right. \\ \quad \left.\left. + \tilde{\alpha}_i I_{i,j}^{n}\right)\varphi_5(S_{i,j}^{n}, I_{i,j}^{n}, P_{i,j}^{n})\right], \end{cases} \tag{27}$$

where

$$\begin{aligned} AP_1 &= 1 + 2\gamma_{s_x} + 2\gamma_{s_y} + \tau\varphi_2(S_{i,j}^{n}, I_{i,j}^{n}) + \tau\varphi_4(I_{i,j}^{n}) + \tau\tilde{\alpha}_s\varphi_5(S_{i,j}^{n}, I_{i,j}^{n}, P_{i,j}^{n}), \\ AP_2 &= 1 + 2\gamma_{i_x} + 2\gamma_{i_y} + \tau\varphi_3(S_{i,j}^{n}, I_{i,j}^{n}) + \tau\tilde{\alpha}_i\varphi_5(S_{i,j}^{n}, I_{i,j}^{n}, P_{i,j}^{n}), \\ AP_3 &= 1 + 2\gamma_{p_x} + 2\gamma_{p_y} + \tau d. \end{aligned}$$

Similarly, the initial and boundary conditions are calculated as method FE-FDM in Subsection 3.1. It can be seen that in the implementation of UPP-FDM, all coefficients in (27) and the parameters of the problem are non-negative, as a result relation (27) produces a non-negative approximation of the solution of the problem without any additional conditions.

4 Consistency of UPP-FDM

The FDM used to approximate a PDE is consistent if the truncation error approaches zero by reducing the time and space subdivisions [43]. In this section, we examine the consistency of UPP-FDM. For this purpose, we first check the consistency of the method for one of the equations of system (4), for example:

$$\partial_t S = \tilde{d}_s\Delta S + \varphi_1(S,I) - \varphi_2(S,I)S - \varphi_4(I)S - \tilde{\alpha}_s\varphi_5(S,I,P)S. \tag{28}$$

Then, we use UPP-FDM for this equation, that is

$$\begin{aligned} S_{i,j}^{n+1}\left[1+2\gamma_{s_x}+2\gamma_{s_y}+\tau\varphi_2(S_{i,j}^n,I_{i,j}^n)+\tau\varphi_4(I_{i,j}^n)+\tilde{\alpha}_s\tau\varphi_5(S_{i,j}^n,I_{i,j}^n,P_{i,j}^n)\right] \\ = S_{i,j}^n+\gamma_{s_x}\left(S_{i+1,j}^n+S_{i-1,j}^n\right)+\gamma_{s_y}\left(S_{i,j+1}^n+S_{i,j-1}^n\right)+\tau\varphi_1(S_{i,j}^n,I_{i,j}^n). \end{aligned} \tag{29}$$

Using Taylor's expansion for $S_{i,j}^{n+1}$, $S_{i+1,j}^n$, $S_{i-1,j}^n$, $S_{i,j+1}^n$ and $S_{i,j-1}^n$, one can get:

$$\begin{aligned} S_{i,j}^{n+1} &= S_{i,j}^n+\tau\frac{\partial S}{\partial t}+\frac{\tau^2}{2!}\frac{\partial^2 S}{\partial t^2}+\frac{\tau^3}{3!}\frac{\partial^3 S}{\partial t^3}+\cdots, \\ S_{i-1,j}^n &= S_{i,j}^n-h_x\frac{\partial S}{\partial x}+\frac{h_x^2}{2!}\frac{\partial^2 S}{\partial x^2}-\frac{h_x^3}{3!}\frac{\partial^3 S}{\partial x^3}+\cdots, \\ S_{i+1,j}^n &= S_{i,j}^n+h_x\frac{\partial S}{\partial x}+\frac{h_x^2}{2!}\frac{\partial^2 S}{\partial x^2}+\frac{h_x^3}{3!}\frac{\partial^3 S}{\partial x^3}+\cdots, \\ S_{i,j-1}^n &= S_{i,j}^n-h_y\frac{\partial S}{\partial y}+\frac{h_y^2}{2!}\frac{\partial^2 S}{\partial y^2}-\frac{h_y^3}{3!}\frac{\partial^3 S}{\partial y^3}+\cdots, \\ S_{i,j+1}^n &= S_{i,j}^n+h_y\frac{\partial S}{\partial y}+\frac{h_y^2}{2!}\frac{\partial^2 S}{\partial y^2}+\frac{h_y^3}{3!}\frac{\partial^3 S}{\partial y^3}+\cdots, \end{aligned}$$

and substituting them into (29) yields:

$$\begin{aligned} &\left(S_{i,j}^n+\tau\frac{\partial S}{\partial t}+\frac{\tau^2}{2!}\frac{\partial^2 S}{\partial t^2}+\frac{\tau^3}{3!}\frac{\partial^3 S}{\partial t^3}+\cdots\right)\left[1+2\frac{\tau\tilde{d}_s}{{h_x}^2}+2\frac{\tau\tilde{d}_s}{{h_y}^2}+\tau\varphi_2(S_{i,j}^n,I_{i,j}^n)+\tau\varphi_4(S_{i,j}^n,I_{i,j}^n)\right. \\ &\left.+\tilde{\alpha}_s\tau\varphi_5(S_{i,j}^n,I_{i,j}^n,P_{i,j}^n)\right]=S_{i,j}^n+\tau\varphi_1(S_{i,j}^n,I_{i,j}^n)+\frac{\tau\tilde{d}_s}{{h_x}^2}\left(S_{i,j}^n+h_x\frac{\partial S}{\partial x}+\frac{h_x^2}{2!}\frac{\partial^2 S}{\partial x^2}+\frac{h_x^3}{3!}\frac{\partial^3 S}{\partial x^3}+\cdots\right. \\ &\left.+S_{i,j}^n-h_x\frac{\partial S}{\partial x}+\frac{h_x^2}{2!}\frac{\partial^2 S}{\partial x^2}-\frac{h_x^3}{3!}\frac{\partial^3 S}{\partial x^3}+\cdots\right)+\frac{\tau\tilde{d}_s}{{h_y}^2}\left(S_{i,j}^n+h_y\frac{\partial S}{\partial y}+\frac{h_y^2}{2!}\frac{\partial^2 S}{\partial y^2}+\frac{h_y^3}{3!}\frac{\partial^3 S}{\partial y^3}+\cdots\right. \\ &\left.+S_{i,j}^n-h_y\frac{\partial S}{\partial y}+\frac{h_y^2}{2!}\frac{\partial^2 S}{\partial y^2}-\frac{h_y^3}{3!}\frac{\partial^3 S}{\partial y^3}+\cdots\right). \end{aligned} \tag{30}$$

Finally, from (30) and (28), the truncation error of the method is obtained as follows:

$$\begin{aligned} T_{i,j}^{n,S} &= \frac{2\tau\tilde{d}_s\frac{\partial S}{\partial t}}{{h_x}^2}+\frac{2\tau\tilde{d}_s\frac{\partial S}{\partial t}}{{h_y}^2}+\frac{\tau\frac{\partial^2 S}{\partial t^2}}{2}+\frac{\tau^2\frac{\partial^3 S}{\partial t^3}}{6}+\frac{\tau^3\frac{\partial^4 S}{\partial t^4}}{24}-\frac{{h_x}^2\tilde{d}_s\frac{\partial^4 S}{\partial x^4}}{12}-\frac{{h_y}^2\tilde{d}_s\frac{\partial^4 S}{\partial y^4}}{12} \\ &+\frac{\tau^2\tilde{d}_s\frac{\partial^2 S}{\partial t^2}}{{h_x}^2}+\frac{\tau^2\tilde{d}_s\frac{\partial^2 S}{\partial t^2}}{{h_y}^2}+\frac{\tau^3\tilde{d}_s\frac{\partial^3 S}{\partial t^3}}{3{h_x}^2}+\frac{\tau^3\tilde{d}_s\frac{\partial^3 S}{\partial t^3}}{3{h_y}^2}+\frac{\tau^4\tilde{d}_s\frac{\partial^4 S}{\partial t^4}}{12{h_x}^2}+\frac{\tau^4\tilde{d}_s\frac{\partial^4 S}{\partial t^4}}{12{h_y}^2}+\cdots. \end{aligned}$$

Choosing $\tau=\min\{h_x^3,h_y^3\}$, if $h_x\to 0$ and $h_y\to 0$, then $T_{i,j}^{n,S}\to 0$. Therefore, (28) is obtained. This process can be developed for the other equations in system (4). Similarly, we can obtain

$$\begin{aligned} T_{i,j}^{n,I} &= \frac{2\tau\tilde{d}_i\frac{\partial I}{\partial t}}{{h_x}^2}+\frac{2\tau\tilde{d}_i\frac{\partial I}{\partial t}}{{h_y}^2}+\frac{\tau\frac{\partial^2 I}{\partial t^2}}{2}+\frac{\tau^2\frac{\partial^3 I}{\partial t^3}}{6}+\frac{\tau^3\frac{\partial^4 I}{\partial t^4}}{24}-\frac{{h_x}^2\tilde{d}_i\frac{\partial^4 I}{\partial x^4}}{12}-\frac{{h_y}^2\tilde{d}_i\frac{\partial^4 I}{\partial y^4}}{12} \\ &+\frac{\tau^2\tilde{d}_i\frac{\partial^2 I}{\partial t^2}}{{h_x}^2}+\frac{\tau^2\tilde{d}_i\frac{\partial^2 I}{\partial t^2}}{{h_y}^2}+\frac{\tau^3\tilde{d}_i\frac{\partial^3 I}{\partial t^3}}{3{h_x}^2}+\frac{\tau^3\tilde{d}_i\frac{\partial^3 I}{\partial t^3}}{3{h_y}^2}+\frac{\tau^4\tilde{d}_i\frac{\partial^4 I}{\partial t^4}}{12{h_x}^2}+\frac{\tau^4\tilde{d}_i\frac{\partial^4 I}{\partial t^4}}{12{h_y}^2}+\cdots, \end{aligned}$$

$$T_{i,j}^{n,P} = \frac{2\tau\tilde{d}_p\frac{\partial P}{\partial t}}{{h_x}^2} + \frac{2\tau\tilde{d}_p\frac{\partial P}{\partial t}}{{h_y}^2} + \frac{\tau\frac{\partial^2 P}{\partial t^2}}{2} + \frac{\tau^2\frac{\partial^3 P}{\partial t^3}}{6} + \frac{\tau^3\frac{\partial^4 P}{\partial t^4}}{24} - \frac{{h_x}^2\tilde{d}_p\frac{\partial^4 P}{\partial x^4}}{12} - \frac{{h_y}^2\tilde{d}_p\frac{\partial^4 P}{\partial y^4}}{12}$$
$$+ \frac{\tau^2\tilde{d}_p\frac{\partial^2 P}{\partial t^2}}{{h_x}^2} + \frac{\tau^2\tilde{d}_p\frac{\partial^2 P}{\partial t^2}}{{h_y}^2} + \frac{\tau^3\tilde{d}_p\frac{\partial^3 P}{\partial t^3}}{3{h_x}^2} + \frac{\tau^3\tilde{d}_p\frac{\partial^3 P}{\partial t^3}}{3{h_x}^2} + \frac{\tau^4\tilde{d}_p\frac{\partial^4 P}{\partial t^4}}{12{h_x}^2} + \frac{\tau^4\tilde{d}_p\frac{\partial^4 P}{\partial t^4}}{12{h_y}^2} + \cdots,$$

where $T_{i,j}^{n,I}$ and $T_{i,j}^{n,P}$ are truncation errors. Selecting $\tau = \min\{h_x^3, h_y^3\}$, if $h_x \to 0$ and $h_y \to 0$, then $T_{i,j}^{n,I} \to 0$ and $T_{i,j}^{n,P} \to 0$. Hence, we have

$$\partial_t I = \tilde{d}_i\Delta I - (\varphi_2(S,I)+\mu)I + \varphi_4(I)S - \tilde{\alpha}_i\varphi_5(S,I,P)I,$$

and

$$\partial_t P = \tilde{d}_p\Delta P - dP + e\left(\tilde{\alpha}_s S + \tilde{\alpha}_i I\right)\varphi_5(S,I,P).$$

Therefore, it can be concluded from what has been said that UPP-FDM is consistent for solving the system (4). Similarly, we can demonstrate the consistency of the FE-FDM and NS-FDM.

5 Stability of UPP-FDM

In this section, we use the von Neumann method to prove the stability of the UPP-FDM. In this method, we check the growth of the initial errors with the help of the Fourier series and thereby obtain the stability conditions of the numerical method [29]. For this purpose, we first consider the small error $E_{l,k}^n = U_{l,k}^n - \tilde{U}_{l,k}^n = e^{\alpha n\tau}e^{i(l\beta_1 h_x + k\beta_2 h_y)} = \xi(t)e^{i(l\beta_1 h_x + k\beta_2 h_y)}$ where $t = n\tau$, l and $k \in \mathbb{R}$, α, β_1 and $\beta_2 \in \mathbb{C}$, $i = \sqrt{-1}$ and $\xi(t) = e^{\alpha t}$ [3]. To simplify calculations, consider the error sentence in form $E_{l,k}^n = \xi(t)e^{i(l\beta_1 h_x + k\beta_2 h_y)}$ and replace it in the system (4). First, we will examine the first equation of system (4). Substituting $S_{l,k}^n = \xi(t)e^{i(l\beta_1 h_x + k\beta_2 h_y)}$ into (29), we have

$$\xi(t+\tau)e^{i(l\beta_1 h_x + k\beta_2 h_y)}\left[1 + 2\gamma_{s_x} + 2\gamma_{s_y} + \tau\varphi_2(S_{i,j}^n, I_{i,j}^n) + \tau\varphi_4(I_{i,j}^n) + \tilde{\alpha}_s\tau\varphi_5(S_{i,j}^n, I_{i,j}^n, P_{i,j}^n)\right]$$
$$= \xi(t)e^{i(l\beta_1 h_x + k\beta_2 h_y)} + \gamma_{s_x}\left(\xi(t)e^{i\left((l+1)\beta_1 h_x + k\beta_2 h_y\right)} + \xi(t)e^{i\left((l-1)\beta_1 h_x + k\beta_2 h_y\right)}\right)$$
$$+ \gamma_{s_y}\left(\xi(t)e^{i\left(l\beta_1 h_x + (k+1)\beta_2 h_y\right)} + \xi(t)e^{i\left(l\beta_1 h_x + (k-1)\beta_2 h_y\right)}\right) + \tau\varphi_1(S_{i,j}^n, I_{i,j}^n),$$

and after rewriting, one can get

$$\xi(t+\tau)\left[1 + 2\gamma_{s_x} + 2\gamma_{s_y} + \tau\varphi_2(S_{i,j}^n, I_{i,j}^n) + \tau\varphi_4(I_{i,j}^n) + \tilde{\alpha}_s\tau\varphi_5(S_{i,j}^n, I_{i,j}^n, P_{i,j}^n)\right]$$
$$= \xi(t)\left[1 + \gamma_{s_x}\left(e^{i\beta_1 h_x} + e^{-i\beta_1 h_x}\right) + \gamma_{s_y}\left(e^{i\beta_2 h_y} + e^{-i\beta_2 h_y}\right)\right].$$

Table 3: Three sets of parameters values to compare the efficiency of the numerical methods FE-FDM, NS-FDM and UPP-FDM

Parameters	$\tilde{r}$	$\tilde{\sigma}$	$\tilde{d}$	$\tilde{\kappa}$	$\tilde{\alpha}_s$	$\tilde{\alpha}_i$	$\tilde{\mu}$	$\tilde{e}$	$\tilde{d}_s$	$\tilde{d}_i$	$\tilde{d}_p$	$\tilde{\rho}_s$	$\tilde{\rho}_i$	$\tilde{\beta}$	$\tilde{\zeta}$
case **(1)**	1	0.3	0.5	0.1	1	1	0.1	1	1	0.2	0.7	0.3	0.3	0.5	0.03
case **(2)**	0.7	0.3	0.2	0.6	1	1	0.5	1	0.5	0.01	0.3	0.2	0.2	0.7	0.7
case **(3)**	0.4	0.7	0.5	0.3	1	1	0.3	1	0.7	0.52	0.6	0.3	0.3	0.5	0.5

Due to the positiveness of the approximate solution produced by the UPP-FDM and triangular inequality, we have

$$\begin{aligned}\left|\frac{\xi(t+\tau)}{\xi(t)}\right| &= \left|\frac{1+2\gamma_{s_x}+2\gamma_{s_y}-4\gamma_{s_x}\sin^2\left(\frac{\beta_1 h_x}{2}\right)-4\gamma_{s_y}\sin^2\left(\frac{\beta_2 h_y}{2}\right)}{1+2\gamma_{s_x}+2\gamma_{s_y}+\tau\varphi_2(S^n_{i,j},I^n_{i,j})+\tau\varphi_4(I^n_{i,j})+\tilde{\alpha}_s\tau\varphi_5(S^n_{i,j},I^n_{i,j},P^n_{i,j})}\right| \\ &= \frac{\left|1+2\gamma_{s_x}+2\gamma_{s_y}-4\gamma_{s_x}\sin^2\left(\frac{\beta_1 h_x}{2}\right)-4\gamma_{s_y}\sin^2\left(\frac{\beta_2 h_y}{2}\right)\right|}{1+2\gamma_{s_x}+2\gamma_{s_y}+\tau\varphi_2(S^n_{i,j},I^n_{i,j})+\tau\varphi_4(I^n_{i,j})+\tau\tilde{\alpha}_s\varphi_5(S^n_{i,j},I^n_{i,j},P^n_{i,j})} \\ &\leqslant \frac{1+2\gamma_{s_x}\left|1-2\sin^2\left(\frac{\beta_1 h_x}{2}\right)\right|+2\gamma_{s_y}\left|1-2\sin^2\left(\frac{\beta_2 h_y}{2}\right)\right|}{1+2\gamma_{s_x}+2\gamma_{s_y}+\tau\varphi_2(S^n_{i,j},I^n_{i,j})+\tau\varphi_4(I^n_{i,j})+\tau\tilde{\alpha}_s\varphi_5(S^n_{i,j},I^n_{i,j},P^n_{i,j})} \\ &\leqslant \frac{1+2\gamma_{s_x}+2\gamma_{s_y}}{1+2\gamma_{s_x}+2\gamma_{s_y}+\tau\varphi_2(S^n_{i,j},I^n_{i,j})+\tau\varphi_4(I^n_{i,j})+\tau\tilde{\alpha}_s\varphi_5(S^n_{i,j},I^n_{i,j},P^n_{i,j})} \leqslant 1.\end{aligned}$$

Similarly, for $I^{n+1}_{l,k}$ and $P^{n+1}_{l,k}$, we can conclude that

$$\begin{aligned}\left|\frac{\xi(t+\tau)}{\xi(t)}\right| &= \left|\frac{1+2\gamma_{i_x}+2\gamma_{i_y}-4\gamma_{i_x}\sin^2\left(\frac{\beta_1 h_x}{2}\right)-4\gamma_{i_y}\sin^2\left(\frac{\beta_2 h_y}{2}\right)}{1+2\gamma_{i_x}+2\gamma_{i_y}+\tau\varphi_3(S^n_{i,j},I^n_{i,j})+\tau\tilde{\alpha}_i\varphi_5(S^n_{i,j},I^n_{i,j},P^n_{i,j})}\right| \\ &\leqslant \frac{1+2\gamma_{i_x}+2\gamma_{i_y}}{1+2\gamma_{i_x}+2\gamma_{i_y}+\tau\varphi_3(S^n_{i,j},I^n_{i,j})+\tau\tilde{\alpha}_i\varphi_5(S^n_{i,j},I^n_{i,j},P^n_{i,j})} \leqslant 1,\end{aligned}$$

and

$$\left|\frac{\xi(t+\tau)}{\xi(t)}\right| = \left|\frac{1+2\gamma_{p_x}+2\gamma_{p_y}-4\gamma_{p_x}\sin^2\left(\frac{\beta_1 h_x}{2}\right)-4\gamma_{p_y}\sin^2\left(\frac{\beta_2 h_y}{2}\right)}{1+2\gamma_{p_x}+2\gamma_{p_y}+\tau d}\right| \leqslant \frac{1+2\gamma_{p_x}+2\gamma_{p_y}}{1+2\gamma_{p_x}+2\gamma_{p_y}+\tau d} \leqslant 1,$$

where $S^n_{i,j}$, $I^n_{i,j}$ and $P^n_{i,j}$ are acted as (local) constants. From the previous inequalities, it can be concluded that UPP-FDM is unconditionally stable, while method the FE-FDM and NS-FDM have not this properties.

6 Numerical simulation and discussion

To compare the numerical methods and their efficiency, we examine the approximate solution of the infected prey with three sets of parameters in Table 3. In Figures 1 and 2, we have solved system (1) using

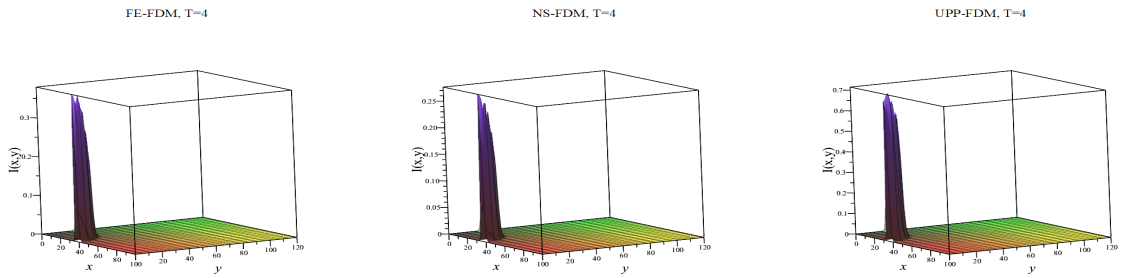

(a) (b) (c)

Figure 1: Density of infected prey for the numerical methods FE-FD, NS-FD and UPP-FD for case **(1)** parameters

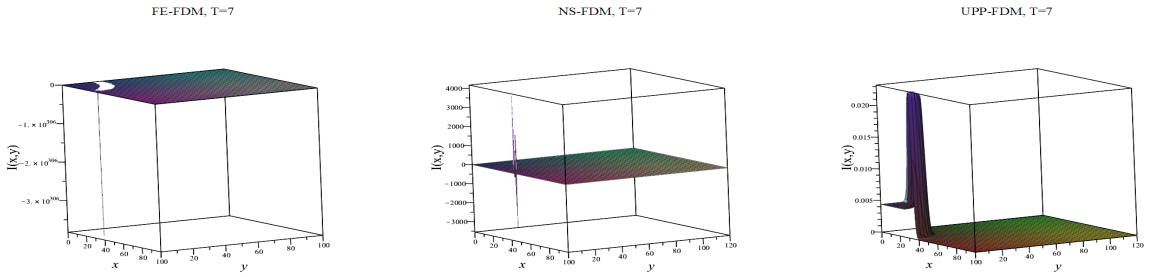

(a) (b) (c)

Figure 2: Density of infected prey for the numerical methods FE-FDM, NS-FDM and UPP-FDM with case **(3)** parameters

three FDMs, namely FE-FDM, NS-FDM, and UPP-FDM. It is important to note that disease outbreaks are always influenced by various factors, such as population density, habitat quality, and appropriate decision-making policies. Therefore, in Figures 1 and 2, the density of the infected population has been examined and compared.

In Figure 1, upon selecting the parameters of case **(1)** at time $t = 4$, it becomes evident that all three numerical methods are capable of producing non-negative approximations. However, in Figure 2, panels **(a)** and **(b)** reveal that the FE-FDM and NS-FDM have generated negative solutions, leading to an incorrect interpretation of disease behavior. In contrast, UPP-FDM offers a more appropriate approximation. Furthermore, in Figure 2, we have chosen the parameters of case **(3)** at time $t = 7$. The approximate solutions of infected prey were compared in all three methods to determine the effectiveness of UPP-FDM in producing non-negative solutions compared to the other two methods. These results are shown in Table 4, where it can be seen that the FE-FDM will fail in large time intervals. If the time and space partitioning are chosen such that condition (24) is met, the NS-FDM will be successful in producing acceptable approximations. Otherwise, this numerical method will not be able to produce non-negative solutions. It should be noted that UPP-FDM not only produces non-negative solutions unconditionally but also uses an acceptable amount of time to calculate these approximations. Figures 3 to 10, are based on UPP-FDM. Panel **(a)** of Figure 3, shows the density of the sensitive prey population, panel

Table 4: The efficiency of the numerical methods FE-FDM, NS-FDM and UPP-FDM in the production of positive answers for infected prey

Case	T	N	M_1	M_2	FE-FDM	NS-FDM	UPP-FDM
case **(1)**	10	50	100	100	✓	✓	✓
case **(2)**	60	60	50	50	×	✓	✓
case **(3)**	10	30	200	200	×	×	✓
CPU time (s) for case **(1)**					22.156	22.281	22.641

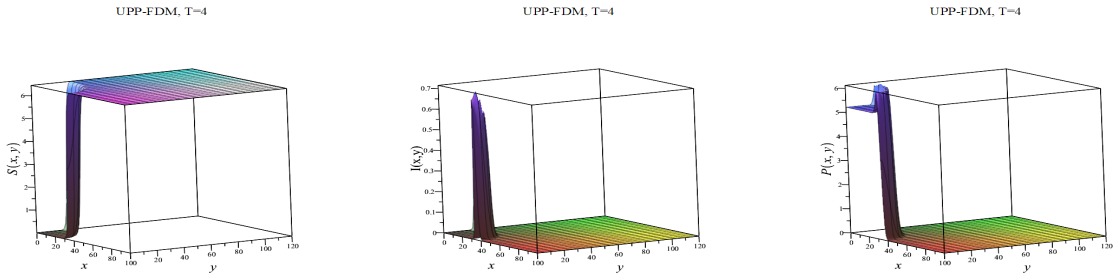

(a) (b) (c)

Figure 3: Approximate solutions with UPP-FDM for case **(1)** parameters

(b) shows the density of the diseased prey population, and panel **(c)** shows the density of the predator population at time $t = 4$. The chosen initial function (32) for the density of the prey and diseased prey species is dense in the area $[0,20] \times [0,30]$ and the density is almost zero outside of this area. In the initial prey operations, the predator was successful in the area $[0,20] \times [0,30]$, and the growth of their population is evident. Also, the disease is transmitted among the prey species outside of this area. However, considering that the predators have negligible dispersion outside of this area at the beginning, the population of prey is significantly increasing. For easier interpretation, contour plots of population densities have been presented in Figures 4, 5, 8, and 9.

Initially, in Figures 4 and 5, we modified the initial function used to solve the system of equations (1) to observe the impact of the initial function on the solution.

Subsequently, based on the outcomes obtained from each initial function, we selected the most suitable one in order to attain better approximations. This selection aims to align our expectations with the achieved approximations for the problem. Both figures include panels **(a)**, depicting the density of the sensitive prey population; **(b)**, illustrating the density of the infected prey population; and **(c)**, showing the density of the predator population at time $t = 50$, utilizing the parameters from case **(3)**.

In these figures, the color yellow signifies the highest population density, transitioning to gradually lighter shades to represent reduced population density. The red color region corresponds to an almost zero population density.

In Figure 4, the initial function is the sigmoid function:

$$f_i(x,y) = a_i + b_i\left(1 - \frac{1}{1+e^{-x+20}}\right)\left(1 - \frac{1}{1+e^{-y+30}}\right), \quad i = 1,2,3, \tag{31}$$

where

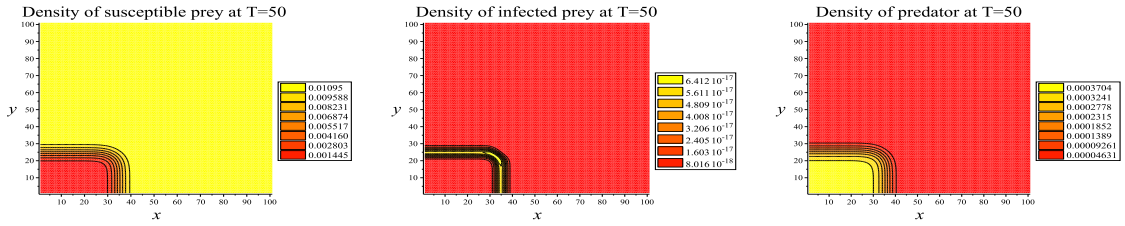

(a) (b) (c)

Figure 4: UPP-FDM contour plot, for case **(3)** parameters with the initial condition of (31)

$$\begin{cases} a_1 = 5, & b_1 = 0, \\ a_2 = 0, & b_2 = 0.3, \\ a_3 = 0, & b_3 = 0.7, \end{cases}$$

and in Figure 5, the initial function is the hyperbolic function:

$$f_i(x,y) = a_i + b_i\big(1 - \tanh(\sqrt{0.4x^2 + 0.9y^2} - 20)\big), \quad i = 1,2,3, \tag{32}$$

where

$$\begin{cases} a_1 = 5, & b_1 = 0, \\ a_2 = 0, & b_2 = 0.6, \\ a_3 = 0, & b_3 = 0.9. \end{cases}$$

As seen in Figure 4, the change in population density is in the form of a rectangle. Panel **(a)** in Figure 4, show the density of the sensitive prey population, which has a very low density due to being hunted by the predators in the rectangular area $[0,30] \times [0,40]$, and the population density gradually increases outside of this area. Panel **(c)** in Figure 4, is located opposite to panel **(a)**. Based on panel **(b)** of Figure 4, in areas $34 < x < 36$ and $24 < y < 26$ and panel **(b)** of Figure 5, in areas $20 < x < 22$ and $35 < y < 37$ diseased prey are more concentrated. Therefore, in the areas mentioned in both figures, the population density of sensitive prey decreases in both figures due to being affected by disease, and the population of predators expands due to the easier capture of diseased prey. The other two panels of Figure 5 provides a similar interpretation of population density but with a radial change in the density region. Considering the unpredictable movement of animal species due to various reasons such as instinctive behavior or natural barriers, the initial function with a radial shape is more relevant to reality. In the subsequent simulations and results, we have used the initial function (32).

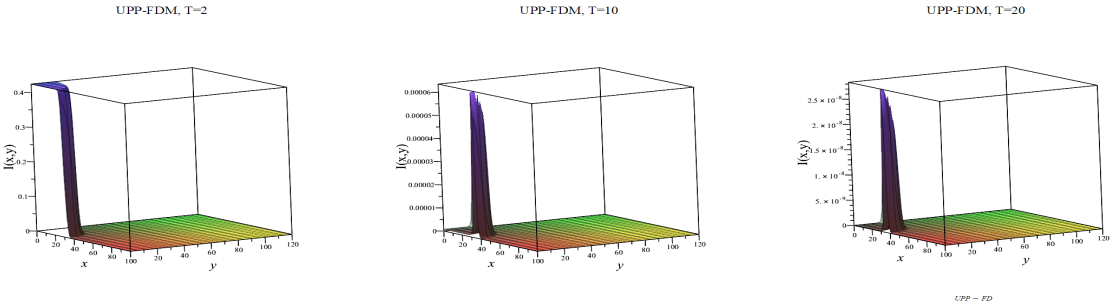

(a) (b) (c)

Figure 6: Density of infected prey with case **(1)** parameters and the initial condition of (32) at T=2, 10, 20

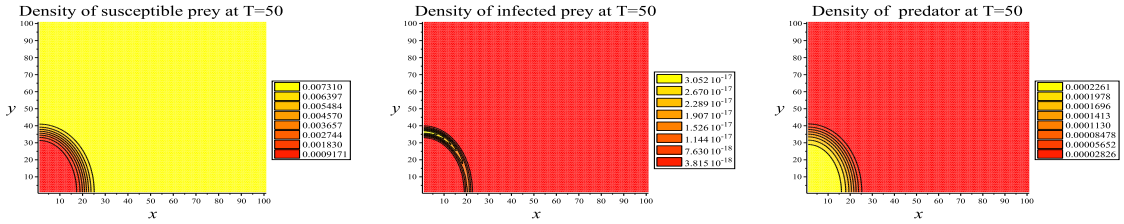

(a) (b) (c)

Figure 5: UPP-FDM contour plot, for case **(3)** parameters with the initial condition of (32)

In Figures 6 and 7, the population density of the diseased prey species is compared at times $t = 2,\ 10,\ 20$. In both figures, it can be observed that the disease will eventually disappear over time. However, the intensity of the disease varies in different areas. In Figure 6, the initial function is (32), and in Figure 7, the initial function is the hyperbolic function:

$$f_i(x,y) = a_i + b_i\big(1 - \tanh(\sqrt{0.02x^2 + 0.9y^2} - 20)\big), \quad i = 1,2,3, \tag{33}$$

where

$$\begin{cases} a_1 = 5, & b_1 = 0, \\ a_2 = 0, & b_2 = 0.6, \\ a_3 = 0, & b_3 = 0.9. \end{cases}$$

The difference between the **x** and **y** coefficients in Figure 6 is much less than in the initial function of Figure 7. Due to a variety of factors, including obstacles in specific areas that impede species movement, the spread of species can vary significantly based on location variables. Therefore, in the presented figures (Figures 8 and 9), we have deliberately selected distinct coefficients **x** and **y** to account for these spatial variations. This distinction is evident in the contour plots depicted in both Figures 8 and 9 where the population density of sensitive prey, infected prey, and predator species is examined using different coefficients in the initial functions (32) and (33) at time $t = 20$. Notably, the reduction of the **x** variable coefficient in Figure 9 leads to a noticeable decrease in species population density along this axis compared to the **y** axis.

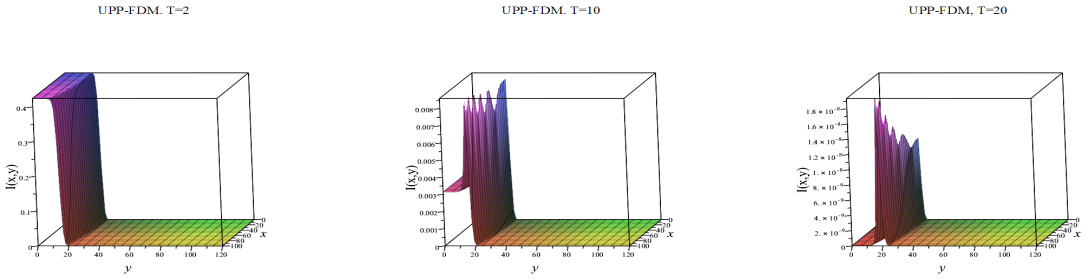

(a) (b) (c)

Figure 7: Density of infected prey with case **(1)** parameters and the initial condition of (33) at T=2, 10, 20

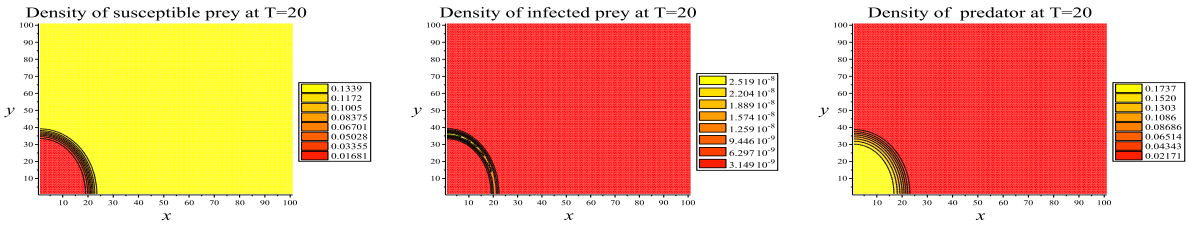

(a) (b) (c)

Figure 8: UPP-FDM contour plot, with case **(3)** parameters and the initial condition of (32)

By choosing the parameters of Section 2, the phase portrait of the dynamic system (1) is shown in Figure 10 about the disease-free and endemic equilibrium points. This figure shows the instability of the disease-free equilibrium point and the stability of the endemic equilibrium point.

7 Conclusion

In our study, we explored the eco-epidemiological model incorporating diffusion and a convex incidence rate model. This choice was motivated by the need to account for the realistic movement patterns of animals within their habitats, which often occur in multiple dimensions. Additionally, animals are typically exposed to diseases either directly or indirectly, further justifying the inclusion of these factors in our research. The summary of the results obtained from this study is as follows:

- The dynamic of system (1) was analyzed by investigating stability conditions concerning the equilibrium points. Furthermore, the stability or instability of these equilibrium points was determined for certain parameters.
- Three numerical methods (FE-FDM, NS-FDM and UPP-FDM) were presented for obtaining the approximate solutions of system (1). We showed that UPP-FDM produces non-negative numerical solutions without any constraint, while the NS-FDM succeeds in generating non-negative solutions under certain conditions. In addition, we observed that the Euler method is often inefficient in computing the non-negative approximations, especially encountered in large time intervals.

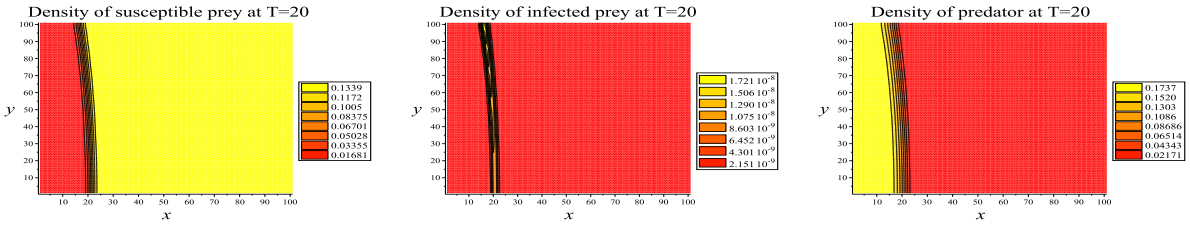

(a) (b) (c)

Figure 9: UPP-FDM contour plot with case **(3)** parameters and the initial condition of (33)

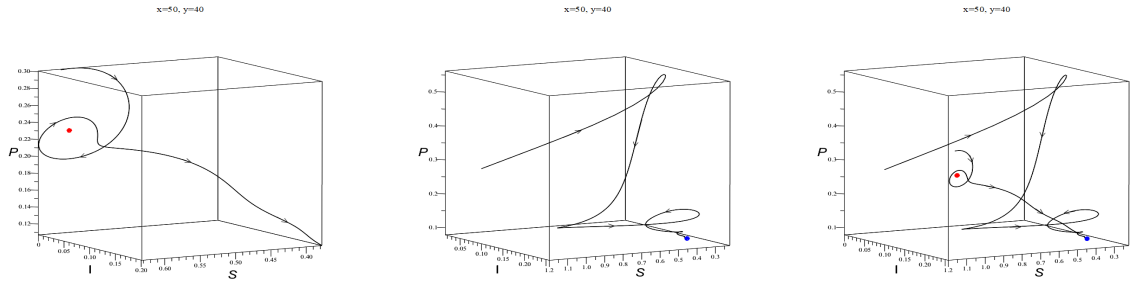

(a) (b) (c)

Figure 10: Phase portrait of the system for disease-free and endemic equilibrium points

- The unconditional consistency and stability of UPP-FDM was proved.

- The effectiveness of generating non-negative approximate solutions through numerical simulations based on three specific parameter sets was demonstrated. Furthermore, analysis was performed on the obtained numerical solutions of the problem, utilizing two different initial conditions (31) and (32). Considering the instincts of animals and their movement in eco-systems, the hyperbolic function (32) was found to be more suitable than the sigmoid function (31) for interpreting the interaction of species with their environment as realistic. These distinctions were explored in Figures 4 and 5. Moreover, through adjustments in the coefficients of **x** and **y** in the hyperbolic function, various predator-prey behaviors in the presence of obstacles were investigated. For instance, the existence of barriers in species movement pathways could result in higher or lower population density along a spatial dimension. This phenomenon is clearly observable in the contour plots (refer to Figures 8 and 9).

In order to further explore the behavior of birds or marine animals, including their defence mechanisms, it is necessary to consider a higher-dimensional space and incorporate different response functions. For future research, we plan to extend the current study to three-dimensional case and incorporate more complex and diverse response functions. This will enable a more comprehensive understanding of the dynamics and interactions of these organisms in their natural habitats.

References

[1] N. Ahmed, S.S. Tahira, M. Rafiq, M.A. Rehman, M. Ali, M.O. Ahmad, *Positivity preserving operator splitting nonstandard finite difference methods for SEIR reaction diffusion model*, Open Math. **17** (2019) 313–330.

[2] N. Ahmed, Z. Wei, D. Baleanu, M. Rafiq, M.A. Rehman, *Spatio-temporal numerical modeling of reaction-diffusion measles epidemic system*, Chaos **29** (2019) 103101.

[3] F. Al-Showaikh, *Numerical modelling of some systems in the biomedical sciences*, Ph.D. thesis, Brunel University, School of Information Systems, Computing and Mathematics, 1998.

[4] J.A. Aledo, C. Andreu-Vilarroig, J.-C. Cortes, J.C. Orengo, R.-J. Villanueva, *On the epidemiological evolution of colistin-resistant acinetobacter baumannii in the city of valencia: An agent-based modelling approach*, Math. Model. Nat. Phenom. **18** (2023) 33.

[5] S. Bagheri, M.H. Akrami, G.B. Loghmani, M. Heydari, *Traveling wave in an eco-epidemiological model with diffusion and convex incidence rate: Dynamics and numerical simulation*, Math. Comput. Simul. **216** (2024) 347–366.

[6] A.M. Bate, F.M. Hilker, *Preytaxis and travelling waves in an eco-epidemiological model*, Bull. Math. Biol. **81** (2019) 995–1030.

[7] B. Buonomo, D. Lacitignola, *On the dynamics of an seir epidemic model with a convex incidence rate*, Ric. Mat. **57** (2008) 261–281.

[8] B. Buonomo, S. Rionero, *On the lyapunov stability for SIRS epidemic models with general nonlinear incidence rate*, Appl. Math. Comput. **217** (2010) 4010–4016.

[9] Y. Cai, Y. Kang, W. Wang, *A stochastic SIRS epidemic model with nonlinear incidence rate*, Appl. Math. Comput. **305** (2017) 221–240.

[10] B.M. Chen-Charpentier, H.V. Kojouharov, *An unconditionally positivity preserving scheme for advection-diffusion reaction equations*, Math. Comput. Model **57** (2013) 2177–2185.

[11] C. Cosner, D.L. DeAngelis, J.S. Ault, D.B. Olson, *Effects of spatial grouping on the functional response of predators*, Theor. Popul. Biol. **56** (1999) 65–75.

[12] K. Dariva, T. Lepoutre, *Influence of the age structure on the stability in a tumor-immune model for chronic myeloid leukemia*, Math. Model. Nat. Phenom. **19** (2024) 1.

[13] R.U. Din, E.A. Algehyne, *Mathematical analysis of COVID-19 by using SIR model with convex incidence rate*, Results Phys. **23** (2021) 103970.

[14] P. Dutta, D. Sahoo, S. Mondal, G. Samanta, *Dynamical complexity of a delay-induced eco-epidemic model with Beddington–DeAngelis incidence rate*, Math. Comput. Simul. **197** (2022) 45–90.

[15] D. Greenhalgh, Q.J. Khan, F.A. Al-Kharousi, *Eco-epidemiological model with fatal disease in the prey*, Nonlinear Anal. Real World Appl. **53** (2020) 103072.

[16] E.E. Holmes, M.A. Lewis, J.E. Banks, R.R. Veit, *Partial differential equations in ecology: spatial interactions and population dynamics*, Ecology **75** (1994) 17–29.

[17] F. Izadi, *Using nonstandard finite difference methods for solving converted schrodinger equation to an ODE*, Iran. J. Optim. **13** (2021) 13–27.

[18] Y. Jin, W. Wang, S. Xiao, *An SIRS model with a nonlinear incidence rate*, Chaos Solit. Fract. **34** (2007) 1482–1497.

[19] A. Khan, R. Zarin, G. Hussain, N.A. Ahmad, M.H. Mohd, A. Yusuf, *Stability analysis and optimal control of covid-19 with convex incidence rate in khyber pakhtunkhawa (pakistan)*, Results Phys. **20** (2021) 103703.

[20] A. Khan, R. Zarin, G. Hussain, A.H. Usman, U.W. Humphries, J.G. Aguilar, *Modeling and sensitivity analysis of HBV epidemic model with convex incidence rate*, Results Phys. **22** (2021) 103836.

[21] A. Korobeinikov, P.K. Maini. *Non-linear incidence and stability of infectious disease models*, Math. Med. Biol. **22** (2005) 113–128.

[22] G.-H. Li, Y.-X. Zhang, *Dynamic behaviors of a modified SIR model in epidemic diseases using nonlinear incidence and recovery rates*, Plos One. **12** (2017) 0175789.

[23] L. Liu, D.P. Clemence, R.E. Mickens, *A nonstandard finite difference scheme for contaminant transport with kinetic langmuir sorption*, Numer. Methods Partial Differ. Equ. **27** (2011) 767–785.

[24] R.E. Mickens, *A best finite-difference scheme for the fisher equation*, Numer. Methods Partial Differ. Equ. **10** (1994) 581–585.

[25] R.E. Mickens, *Exact solutions to a finite-difference model of a nonlinear reaction-advection equation: Implications for numerical analysis*, Numer. Methods Partial Differ. Equ. **5** (1989) 313–325.

[26] A. Mondal, A.K. Pal, G.P. Samanta, *Analysis of a delayed eco-epidemiological pest–plant model with infected pest*, Biophys Rev. Lett. **14** (2019) 141–170.

[27] A. Mondal, A. Pal, G. Samanta, *On the dynamics of evolutionary leslie-gower predator-prey eco-epidemiological model with disease in predator*, Ecol. Genet. Genom. **10** (2019) 100034.

[28] J.D. Murray, *Mathematical Biology: II: Spatial Models and Biomedical Applications*, volume 3. Springer, 2003.

[29] A. Nauman, M. Rafiq, M.A. Rehman, M. Ali, M.O. Ahmad, *Numerical modeling of seir measles dynamics with diffusion*, Commun. Math. Appl. **9** (2018) 315.

[30] A. Pal, A. Bhattacharyya, A. Mondal, *Qualitative analysis and control of predator switching on an eco-epidemiological model with prey refuge and harvesting*, Results Control Optim. **7** (2022) 100099.

[31] A.K. Pal, A. Bhattacharyya, A. Mondal, S. Pal, *Qualitative analysis of an eco-epidemiological model with a role of prey and predator harvesting*, Z. Naturforsch. A. **77** (2022) 629–645.

[32] A. Pal, G. Samanta, *Stability analysis of an eco-epidemiological model incorporating a prey refuge*, Nonlinear Anal. Model. Control **15** (2010) 473–491.

[33] M.S. Rahman, S. Chakravarty, *A predator-prey model with disease in prey*, Nonlinear Anal. Model. Control **18** (2013) 191–209.

[34] G.U. Rahman, K. Shah, F. Haq, N. Ahmad, *Host vector dynamics of pine wilt disease model with convex incidence rate*, Chaos Solit. Fract. **113** (2018) 31–39.

[35] L.-I.W. Roeger, *Dynamically consistent discrete-time SI and SIS epidemic models*, Conf. Publ. **2013** (2013) 653–662.

[36] S. Saha, A. Maiti, G.P. Samanta, *A Michaelis–Menten predator–prey model with strong Allee effect and disease in prey incorporating prey refuge*, Int. J. Bifurc. Chaos **28** (2018) 1850073.

[37] S. Saha, G.P. Samanta, *A prey-predator system with disease in prey and cooperative hunting strategy in predator*, J. Phys. A: Math. Theor. **53** (2020) 485601.

[38] G. Samanta, *Deterministic, Stochastic and Thermodynamic Modelling of some Interacting Species*, Forum for Interdisciplinary Mathematics. Springer Singapore, 2021.

[39] X.-F. San, Z.-C. Wang, Z. Feng, *Spreading speed and traveling waves for an epidemic model in a periodic patchy environment*, Commun. Nonlinear Sci. Numer. Simul. **90** (2020) 10538.

[40] N. Santra, S. Saha, G. Samanta, *Exploring cooperative hunting dynamics and prcc analysis: insights* J. Phys. A: Math. Theor. **57** (2024) 305601.

[41] N. Sapoukhina, Y. Tyutyunov, R. Arditi, *The role of prey taxis in biological control: a spatial theoretical model*, Am. Nat. **162** (2003) 61–76.

[42] M. Sieber, H. Malchow, F.M. Hilker, *Disease-induced modification of prey competition in eco-epidemiological models*, Ecol. Complex. **18** (2014) 74–82.

[43] G.D. Smith, *Numerical solution of partial differential equations: finite difference methods*, Oxford University Press, 1985.

[44] H. Yang, Y. Wang, S. Kundu, Z. Song, Z. Zhang, *Dynamics of an SIR epidemic model incorporating time delay and convex incidence rate*, Results Phys. **32** (2022) 105025.